doi:10.1093/brain/awz105 BRAIN 2019: 142; 1535–1546 | 1535

BRAIN
A JOURNAL OF NEUROLOGY

REPORT

Loss of $STEP_{61}$ couples disinhibition to *N*-methyl-D-aspartate receptor potentiation in rodent and human spinal pain processing

Annemarie Dedek,[1,2,*] Jian Xu,[3,*] Chaya M. Kandegedara,[1,2] Louis-Étienne Lorenzo,[4] Antoine G. Godin,[4,5] Yves De Koninck,[4,5,6] Paul J. Lombroso,[3] Eve C. Tsai[2,7] and Michael E. Hildebrand[1,2,7]

*These authors contributed equally to this work.

Dysregulated excitability within the spinal dorsal horn is a critical mediator of chronic pain. In the rodent nerve injury model of neuropathic pain, BDNF-mediated loss of inhibition (disinhibition) gates the potentiation of excitatory GluN2B *N*-methyl-D-aspartate receptor (NMDAR) responses at lamina I dorsal horn synapses. However, the centrality of this mechanism across pain states and species, as well as the molecular linker involved, remain unknown. Here, we show that KCC2-dependent disinhibition is coupled to increased GluN2B-mediated synaptic NMDAR responses in a rodent model of inflammatory pain, with an associated downregulation of the tyrosine phosphatase $STEP_{61}$. The decreased activity of $STEP_{61}$ is both necessary and sufficient to prime subsequent phosphorylation and potentiation of GluN2B NMDAR by BDNF at lamina I synapses. Blocking disinhibition reversed the downregulation of $STEP_{61}$ as well as inflammation-mediated behavioural hypersensitivity. For the first time, we characterize GluN2B-mediated NMDAR responses at human lamina I synapses and show that a human *ex vivo* BDNF model of pathological pain processing downregulates KCC2 and $STEP_{61}$ and upregulates phosphorylated GluN2B at dorsal horn synapses. Our results demonstrate that $STEP_{61}$ is the molecular brake that is lost following KCC2-dependent disinhibition and that the decrease in $STEP_{61}$ activity drives the potentiation of excitatory GluN2B NMDAR responses in rodent and human models of pathological pain. The *ex vivo* human BDNF model may thus form a translational bridge between rodents and humans for identification and validation of novel molecular pain targets.

1 Department of Neuroscience, Carleton University, Ottawa, ON, Canada
2 Neuroscience Program, Ottawa Hospital Research Institute, Ottawa, ON, Canada
3 Child Study Center, Yale University School of Medicine, New Haven, CT, USA
4 CERVO Brain Research Centre, Quebec Mental Health Institute, Quebec, QC, Canada
5 Department of Psychiatry and Neuroscience, Université Laval, Quebec, QC, Canada
6 Graduate Program in Neurobiology, Université Laval, Quebec, QC, Canada
7 Brain and Mind Research Institute, University of Ottawa, Ottawa, ON, Canada

Correspondence to: Michael E. Hildebrand
Department of Neuroscience, Carleton University, Ottawa, ON, Canada
E-mail: Mike.Hildebrand@carleton.ca

Keywords: pain; spinal cord; NMDAR; KCC2; $STEP_{61}$

Abbreviations: CFA = complete Freund's adjuvant; mEPSCs = miniature excitatory postsynaptic currents; NMDAR = *N*-methyl-D-aspartate receptor

Received September 24, 2018. Revised February 4, 2019. Accepted February 25, 2019

Introduction

Chronic pain is a widespread, debilitating disease with few safe and effective treatments. To develop novel therapeutic approaches, we must identify the molecular determinants of pathological pain (Gereau *et al.*, 2014; Yekkirala *et al.*, 2017). However, the vast majority of basic science pain research ends at target identification and validation in rodent models of chronic pain. Typically, findings from rodent models form the scientific rationale for a large jump to direct testing of individual compounds in specific human pain syndromes. When candidate molecules fail in clinical testing, their targets are often abandoned even when the underlying reasons for failure remain unexplored (Morgan *et al.*, 2012). Thus, proof-of-concept human tissue studies are urgently needed to test assumptions on cross-species similarity and to bridge the rodent-to-human translational divide (Gereau *et al.*, 2014).

Pathological pain arises when neurons in the nociceptive pathway become sensitized by repeated exposure to noxious stimuli. Within the spinal dorsal horn, sensitization disrupts the balance between excitation and inhibition, leading to a sustained increase in nociceptive transmission from lamina I output neurons to the brain (Latremoliere and Woolf, 2009; Todd, 2010; Bourinet *et al.*, 2014; Kuner, 2015; Alles and Smith, 2018). We have recently found that two mechanisms of dorsal horn hyperexcitability—BDNF-mediated disinhibition (Coull *et al.*, 2005) and GluN2B *N*-methyl-D-aspartate receptor (NMDAR) potentiation by the Src family kinase, Fyn (Abe *et al.*, 2005)—are directly linked following nerve injury (Hildebrand *et al.*, 2016). However, the molecular linker that drives the coupling between disinhibition and facilitated excitation remains unidentified. Here, we investigate this critical problem in both rodent and human spinal models of pathological pain.

Materials and methods

Animals

All rodent experiments were performed on male adult Sprague-Dawley rats supplied by Charles River Laboratories, weighing 350–450 g. Animals were housed and cared for in accordance with the recommendations of the Canadian Council for Animal Care and from regulations and policies of Carleton University and the University of Ottawa Heart Institute. Animals were housed in pairs, had free access to food and water and were randomly assigned to their respective experimental groups.

Freund's adjuvant model of inflammatory pain and behaviour testing

Complete Freund's adjuvant (CFA, Sigma) was used to model inflammatory pain. Rats were given a 0.4 ml plantar injection of either phosphate-buffered saline (PBS: control) or CFA (a 50% by volume mixture of CFA and PBS) under isoflurane anaesthesia.

Behaviour testing for pain hypersensitivity was performed using von Frey filaments to measure mechanical paw withdrawal threshold. Withdrawal threshold was measured using the simplified up-down method (SUDO), as described by Bonin *et al* (2014). The SUDO method standardizes the number of stimuli per test to five, thus ensuring that each animal receives a constant number of trials while minimizing the number of stimuli to prevent sensitization during testing. Measurements were taken at baseline (pre-injection), and then every 24 h until the end-point of the study. Animals used for biochemical analysis were sacrificed 120 h post-CFA injection. Animals used for electrophysiological recording were sacrificed 72–120 h post-CFA injection. For both biochemical analysis and electrophysiological recording, only the ipsilateral side of the lumbar spinal cord was used.

Intraperitoneal injection of acetazolamide

Seventy-two hours following sub-plantar injection of CFA and following behaviour testing (see above), male Sprague-Dawley rats were given an intraperitoneal injection of 300 mg/kg acetazolamide (Sigma) dissolved in Ringer's solution (pH 8.28). Behaviour testing was then performed every 10 min, with the experimenter blinded to treatment conditions. A small pilot of 10 animals was used to identify the time point of maximal behaviour reversal, which was 40 min post-intraperitoneal injection. All further cohorts were sacrificed after the behaviour testing at 40 min post-intraperitoneal injection.

Rat spinal cord isolation

Rats were anaesthetized using an intraperitoneal injection of 3 g/kg urethane (Sigma). Once under deep anaesthesia, spinal cords were rapidly dissected via ventral laminectomy and immediately placed in ice-cold oxygenated protective sucrose artificial CSF solution (referred to as 'saline': 50 mM sucrose, 92 mM NaCl, 15 mM D-glucose, 26 mM $NaHCO_3$, 5 mM KCl, 1.25 mM NaH_2PO_4, 0.5 mM $CaCl_2$, 7 mM $MgSO_4$, 1 mM kynurenic acid, bubbled with 5% CO_2/95% O_2). The L3–L6 lumbar region was isolated and dorsal and ventral roots were removed under a dissection microscope.

The spinal cords were then sliced parasagittally to 300 µm for electrophysiological recording using a Leica VT1200S vibratome at an amplitude of 2.75 mm and a speed of 0.1 mm/s through the dorsal horn. Kynurenic acid was washed out by incubating slices in 34°C, kynurenic acid-free saline for 40 min. Previous control experiments have shown no difference in NMDAR synaptic responses in lamina I neurons from slices that were sectioned in saline with or without kynurenic acid as long as slices were recovered in kynurenic acid-free saline (data not shown). Following this recovery period, the incubation chamber was removed from the heated water bath and allowed to cool to room temperature. For biochemical analysis, a ~400 µm horizontal section containing the dorsal horn was removed. The following 1200 µm of spinal tissue containing the deep dorsal horn and ventral horn was used for control comparisons. Following slicing,

tissue for biochemical analysis was either flash frozen using histo-freeze (Fisher Super Friendly Freeze'It) or was treated according to the *ex vivo* model of pathological pain processing (see below) and then flash frozen.

Human spinal cord preparation

Spinal tissue was collected from adult (18–69-years-old) male human organ donors identified by the Trillium Gift of Life Network. Donors were pre-screened to exclude patients with communicable diseases (hepatitis, HIV/AIDS or syphilis) or chronic conditions such as morbid obesity that could negatively affect health of the donor's organs. Tissue from donors that had spinal cord damage or that were taking chronic pain medications were also excluded from the study. The most common cause of death was compromised blood flow to the brain (haemorrhage or ischaemia). For the collection and experimentation with human spinal cord tissue, approval was obtained from the Ottawa Health Science Network Research Ethics Board. Hypothermia was induced using a cooling bed and the body was perfused with high magnesium protective solution (Celsior or Belzer UW) before organ collection. Spinal cords were isolated via ventral laminectomy within 114 ± 25 min (n = 14) of cross-clamping the heart, after organs were removed for donation. Once the spinal cord was removed, the thoracic and lumbar regions were isolated and placed in ice-cold saline in preparation for biochemical, immunohistochemical and/or electrophysiological experiments. A summary of which experimental procedures were performed on each human spinal cord sample can be found in Supplementary Table 1.

In a subset of donors, human spinal tissue for electrophysiological recording was sectioned in the transverse plane into 400–500 µm sections using a Leica vibratome at an amplitude of 2.75 mm and a speed of 0.1 mm/s through the dorsal horn. As done for rodent slices, spinal sectioning was performed in oxygenated, ice-cold saline including 1 mM kynurenic acid, followed by recovery in saline without kynurenic acid at 34°C for 40 min. Human tissue for biochemical analysis was left unsectioned and was treated according to the *ex vivo* model of pathological pain processing (see below). Following treatment according to the *ex vivo* model, tissue was either flash-frozen, and the dorsal horn was removed using a scalpel blade or tissue was fixed with 4% paraformaldehyde.

Ex vivo model of pathological pain processing

Following removal of the spinal cord from the subject (rat or human) according to the above-stated procedures, tissue was placed in oxygenated, room temperature saline containing 50–100 ng/ml recombinant BDNF (Alomone Labs) or saline alone for 70–80 min. This same approach was used for treatment of spinal tissue with BDNF and TAT-STEP, BDNF and acetazolamide, acetazolamide alone, or TC-2153.

Electrophysiological recordings of lamina I neurons

After slice preparation, cells were viewed using brightfield optics. Lamina I neurons were located dorsal to the substantia gelatinosa, within the 50 µm portion of tissue directly ventral of the white matter. As described previously (Hildebrand *et al.*, 2016), the extracellular recording solution used was an artificial CSF solution containing (in mM): 125 NaCl, 20 D-glucose, 26 $NaHCO_3$, 3 KCl, 1.25 NaH_2PO_4, 2 $CaCl_2$, and 1 $MgCl_2$ in addition to 500 nM TTX, 10 µM Cd^{2+}, 10 µM strychnine and 10 µM bicuculline to block voltage-gated Na^+ channel, voltage-gated Ca^{2+} channel, glycinergic and GABAergic currents, respectively. We used borosilicate glass patch-clamp pipettes with resistances of 6–12 MΩ. The internal patch pipette solution contained (in mM): 105 Cs-gluconate, 17.5 CsCl, 10 BAPTA or 10 EGTA, 10 HEPES, 2 MgATP, 0.5 Na_2GTP and had a pH of 7.25 and an osmolarity of 295 mOsm.

Criteria for recorded neurons were as follows: an access resistance below 30 MΩ, and leakage currents less than −100 pA at a holding potential (V_h) of −70 mV. We also selected for the larger neurons in the area, to favour projection neurons. After establishing a whole-cell patch at −60 mV, the holding potential was slowly increased to +60 mV to record NMDAR miniature excitatory postsynaptic currents (mEPSCs). Selection criteria for mEPSCs included: no events that completely decay within 100 ms, no outlier events with an amplitude >100 pA for rat cells and 200 pA for human cells, and events must decay to at least 50% of their overall amplitude by 500 ms. For analysis, mEPSC traces were detected and averaged together for each given treatment in Clampfit 10.7 (Molecular Devices). Traces were then transferred to Origin Pro (Northampton) for graphing.

Isolation of synaptosome fractions and biochemical analysis of human and rodent spinal cord tissue

The human spinal cord was treated according to the *ex vivo* model of pathological pain processing following tissue collection. The tissue was flash-frozen with liquid nitrogen following treatment and stored at −80°C. Approximately 4 mm of the superficial dorsal horn was separated from the rest of the cord using a scalpel blade on dry ice. For rats, the lumbar region of the rat spinal cord was sectioned using a vibratome to obtain a ∼400 µm superficial dorsal horn section and another section consisting of the remainder of the spinal cord.

The isolation of synaptosomal fractions was performed as described previously (Xu *et al.*, 2009). Tissue was first homogenized using Wheaton dounce tissue grinders in 300 µl of ice-cold TEVP-320 mM sucrose buffer containing (in mM): 320 sucrose, 10 Tris-HCl (pH 7.4), 1 EDTA, 1 EGTA, 5 NaF, and 1 Na_3VO_4 with complete protease inhibitor and phosphatase inhibitor cocktails (Roche) to obtain total homogenates. A fraction of the homogenates was used for analysis. The remaining total homogenate lysates were centrifuged at 4°C for 10 min at 1000g and a further 15 min at 12 000g to obtain the crude synaptosome pellet. The pellet was resuspended in TEVP 320 mM sucrose buffer by brief sonication.

The protein content of the homogenates and the synaptosomal fractions was determined by the Pierce BCA protein assay kit (Thermo Scientific). Thirty micrograms of total protein from each sample were loaded on 8% SDS-PAGE and transferred to PVDF membranes (Bio-Rad).

Membranes were blocked in 5% bovine serum albumin (BSA) in Tris-buffered saline (TBS) + 0.1% TWEEN-20

(TBS-T) and incubated overnight in 5% BSA + TBS-T plus primary antibodies [anti-STEP (1:1000), anti-KCC2 (1:1000), anti-Fyn (1:1000) and anti-β-actin (1:10 000) from Santa Cruz; anti-non-phospho-STEP (1:1000) and anti-pY416-Src (or pY420-Fyn) (1:1000) from Cell Signaling; anti-pY1472GluN2B (1:1000) and anti-pY1325GluN2A (1:1000) from PhosphoSolutions; anti-GluN2B (1:2000) and anti-GluN2A (1:1000) from Millipore; for further details on antibodies used in western blots, see Supplementary Table 2]. Membranes were washed three times with TBS-T and incubated in horseradish peroxidase (HRP)-conjugated secondary antibodies (anti-mouse and anti-rabbit (1:5000) from Pierce for 2 h at room temperature. Membranes were developed using Chemiluminescent Substrate kit (Pierce) and visualized using G:BOX with the GeneSnap software (Syngene). All densitometric bands were quantified using ImageJ (NIH).

Immunohistochemistry and antibodies

Transverse fixed human spinal sections were cut at 25 µm on a sledge freezing microtome Leica SM2000R (Leica Microsystems). Sections were permeabilized in PBS (pH 7.4) with 0.2% Triton (PBS+T) for 10 min, washed twice in PBS and incubated for 12 h at 4°C in primary anti-KCC2 antibody and anti-CGRP antibody (see below) diluted in PBS+T containing 10% normal goat serum. After washing in PBS, the tissue was incubated for 2 h at room temperature in a solution containing a mixture of the goat-Cy3 anti-rabbit purified secondary antibody (1:500, Jackson ImmunoResearch Laboratories, Cat. #111–165–144) goat anti-mouse Alexa Fluor® 647 cross-adsorbed secondary antibody (1:500, Thermo Fisher Scientific Cat. #A-21235) and DAPI (1:500, Thermo Fisher Scientific; Cat. #D1306) diluted in PBS+T (pH 7.4) containing 10% normal goat serum. Sections were mounted on SuperFrost™ gelatin-subbed slides (Fisherbrand) and cover-slipped using fluorescence mounting medium (Dako, Cat. #S3023).

Markers of the peptidergic small diameter afferent terminals

Calcitonin gene-related peptide (CGRP) immunoreactivity was used as a specific marker of nociceptive peptidergic afferent terminals (not present in any other types of axons in the dorsal horn) (Rosenfeld *et al.*, 1983; Gibson *et al.*, 1984; Hunt and Rossi, 1985; Ju *et al.*, 1987) using a monoclonal anti-CGRP antibody (1:5000; Sigma #C7113) raised in mouse. This antiserum detects human α-CGRP and β-CGRP but does not cross-react with any other peptide (data supplied by Sigma).

Anti-KCC2 antibody

A polyclonal antibody raised in rabbit (1:1000, Millipore/Upstate, Cat. #07–432) was used in this study. This antibody was raised against a His-tag fusion protein corresponding to residues 932–1043 of the rat KCC2 intracellular C-terminal (Williams *et al.*, 1999; Mercado *et al.*, 2006). This antibody is highly specific for rat KCC2 (KCC2a and KCC2b isoforms) and does not share any homologous sequences with other KCCs or co-transporters.

Confocal laser scanning microscopy

All confocal images were acquired using a Zeiss LSM 880 Confocal Laser Scanning Microscope. Acquisitions were 12-bit images of size 2048 × 2048 pixels with a pixel dwell time of 10 µs. An oil-immersion ×63 plan-apochromatic objective was used for high magnification confocal laser scanning microscopy images, which were processed for quantification. Laser power was adequately chosen to avoid saturation and limit photobleaching. All the acquisitions were performed with the same laser settings [laser, power, photomultiplier tube (PMT) settings, image size, pixel size and scanning time]. During the acquisitions, the experimenter was blind to the slice conditions (i.e. saline versus BDNF treatment).

Ex vivo subcellular KCC2 distribution in human dorsal horn neurons

We developed homemade MATLAB routines to quantify and monitor the changes in the KCC2 intensity distributions in subcellular compartments. This new method is based on a modified version of an already published algorithm used to detect receptor membrane internalization (Ferrini *et al.*, 2017). A user has to delineate the membrane of neuronal cell bodies present in the acquired confocal image. For this analysis, we use CGRP as a marker of the superficial dorsal horn. Only neurons present in the regions of the dorsal horn expressing CGRP were considered. The imaging and analysis were both done blind to the experimental conditions. For each pixel in the region of interest, the distance to the closest membrane segment was calculated. Using this distance map, the mean pixel intensity and standard deviation of KCC2 fluorescence signal were quantified as a function of the distance to the neuron membrane. A negative position value represents the region outside of the labelled neuron. A total of 118 neurons for saline and 108 neurons for BDNF from nine adult males were analysed. Two types of cells were observed during the analysis. The first type showed a strong membrane staining, while the other type exhibited a larger intracellular KCC2 labelling. Because of this, we divided all analysed cells into two groups using the position of the maximum KCC2 intensity in each subcellular profile. Cells for which the KCC2 intensity maximum was at a distance <0.5 µm and >0.5 µm were pooled in two distinct groups. For saline, 108/116 neurons are in the first group (<0.5 µm); in contrast, 36 of 108 neurons analysed for the BDNF conditions are in the second group (>0.5 µm). Averaged profiles were obtained for each subject and condition (saline and BDNF) and from those averages, the global KCC2 intensity profiles were obtained for each condition. The KCC2 membrane intensity (at position 0 µm) and the KCC2 intracellular intensity (0.5 µm $<$ position <2.5 µm) were extracted from each subject's averaged KCC2 intensity profiles. We carried out 2-way parametric paired *t*-tests on the KCC2 intensity at the membrane and in the intracellular compartment and a χ^2 test to test the statistical difference between the distributions of cells in the two conditions.

Statistical analysis

All data are presented as means ± standard error of the mean (SEM). Comparison of means were performed using Student's paired and unpaired *t*-tests (Microsoft Excel Office 365), and

one-way ANOVAs (IBM SPSS Statistics 25.0). Tukey's significant difference test followed ANOVAs, as appropriate. A Pearson's χ^2 test was used in Supplementary Fig. 7D. In all tests, $P < 0.05$ were considered statistically significant. Supplementary Table 3 lists all tests performed, the comparison made, and the associated *P*-values.

Data availability

The authors confirm that the data supporting the findings of this study are available within the article and its Supplementary material.

Results

To test whether NMDAR responses at lamina I synapses are potentiated across pathological pain models, we measured mEPSCs in adult male rats that received a hind-paw injection of CFA. The CFA injection model of persistent inflammation induces prolonged pain hypersensitivity that is mediated by dorsal horn sensitization (Ren *et al.*, 1992). We selected rats that had a sustained reduction in withdrawal threshold of the ipsilateral paw 3–5 days after CFA injection (Fig. 1A). As observed for the nerve injury model (Hildebrand *et al.*, 2016), we found that the NMDAR component of mEPSCs in lamina I neurons was significantly increased in CFA injected rats (NMDAR charge transfer = 6.54 ± 0.32 pC, $n = 8$ neurons from six animals) compared to naïve rats (NMDAR charge transfer = 3.01 ± 0.18 pC, $n = 10$ neurons from eight animals, $P = 2.92 \times 10^{-8}$) (Fig. 1B and Supplementary Table 3). Moreover, the component of NMDAR mEPSCs that was potentiated in CFA-injected rats compared to naïve rats had a decay constant of 210 ms, which is consistent with GluN2B-mediated NMDAR responses (Hildebrand *et al.*, 2014). GluN2B-containing NMDARs are potentiated by Fyn-dependent phosphorylation at Tyr^{1472}, while Fyn itself is activated by phosphorylation at Tyr^{420} (Trepanier *et al.*, 2012). To test for CFA-induced changes in total and phosphorylated levels of GluN2B and Fyn, we performed western blot analysis on the crude synaptosomal fraction of the superficial dorsal horn. As found in the nerve injury model (Hildebrand *et al.*, 2016), CFA injection led to a significant increase in activated (pY^{420}, $P = 0.032$) but not total ($P = 0.42$) Fyn and an associated increase in total ($P = 0.047$) and phosphorylated (pY^{1472}, $P = 0.016$) GluN2B in superficial dorsal horn synaptosomes ($n = 4$; Fig. 1C and Supplementary Table 3).

The BDNF-dependent disinhibition of lamina I neurons is mediated by a downregulation of the KCC2 chloride transporter and subsequent loss of the chloride gradient required for $GABA_A$-dependent synaptic inhibition (Coull *et al.*, 2005). We found that KCC2 was significantly decreased in superficial dorsal horn synaptosomes following CFA injection ($n = 4$, $P = 0.023$; Fig. 1C). We also found that KCC2 ($P = 0.0064$) was downregulated and pY^{420} Fyn ($P = 0.0011$) as well as total ($P = 0.026$) and pY^{1472} GluN2B ($P = 0.016$) were upregulated in the *ex vivo* BDNF model of pathological pain processing ($n = 8$; Fig. 1D and Supplementary Table 3), where spinal sections from naïve rats are treated with recombinant (50 ng/ml) BDNF (Coull *et al.*, 2005; Hildebrand *et al.*, 2016) (Fig. 2A). The KCC2-Fyn-GluN2B signalling pathway was restricted to superficial dorsal horn synaptosomes, as no BDNF-mediated changes were observed in either the homogenate fraction of superficial dorsal horn (Supplementary Fig. 1) nor in the synaptosome fraction of the remainder of the spinal cord (Supplementary Fig. 2). Taken together, our results show that GluN2B-containing NMDARs are phosphorylated and potentiated by a KCC2- and Fyn-dependent pathway at lamina I synapses in CFA-injected rodents. We therefore propose that KCC2-dependent disinhibition is coupled to NMDAR potentiation in both neuropathic (Hildebrand *et al.*, 2016) and inflammatory models of chronic pain. However, what is the molecular linker that couples these two distinct pathological mechanisms?

We have shown that the protein tyrosine phosphatase $STEP_{61}$ promotes dephosphorylation and inactivation of Fyn (at pY^{420}) and that BDNF signalling leads to the degradation of $STEP_{61}$ at brain synapses (Xu *et al.*, 2015*a*; Saavedra *et al.*, 2016). Interestingly, we found here that active (dephosphorylated at Ser^{221}) $STEP_{61}$ was significantly decreased in superficial dorsal horn synaptosomes in the *in vivo* CFA and *ex vivo* BDNF models of pathological pain processing ($n = 4$, $P = 0.036$, Fig. 1C; $n = 8$, $P = 0.013$; Fig. 1D). To test whether $STEP_{61}$ downregulation is required for the potentiation of NMDAR responses at lamina I synapses, we co-treated spinal sections of naïve rats with both recombinant BDNF and a fusion peptide that contained a membrane-permeable TAT domain followed by the active STEP peptide (TAT-STEP) (Paul *et al.*, 2007; Xu *et al.*, 2009). Co-treatment of TAT-STEP (200 nM) with BDNF ($n = 6$) prevented the potentiation of NMDAR mEPSCs observed in neurons treated with BDNF and a TAT-fusion control peptide (200 nM, $n = 7$, $P = 6.3 \times 10^{-4}$; Fig. 2B). The NMDAR charge transfer for neurons treated with BDNF and TAT-STEP was not significantly different from that of neurons in untreated spinal sections ($n = 8$, $P = 0.28$; Fig. 2B), demonstrating that restoring STEP activity completely abolishes the BDNF-mediated potentiation of NMDAR responses at lamina I synapses. We next used the small organic STEP inhibitor, TC-2153 (Xu *et al.*, 2014), to test whether blocking STEP activity itself is sufficient to induce potentiation of synaptic NMDAR responses. Pretreating spinal sections from naïve rats with TC-2153 (1 μM, $n = 9$) did not significantly alter NMDAR mEPSCs compared to control saline-treated slices ($n = 6$, $P = 0.33$; Fig. 2C). However, following slice pretreatment with TC-2153, administration of BDNF during recording significantly increased synaptic NMDAR responses ($n = 7$, $P = 0.028$; Fig. 2D). Perfusion of BDNF had no effect on NMDAR mEPSCs in saline pretreated slices ($n = 6$, $P = 0.97$). Similar to previous experiments

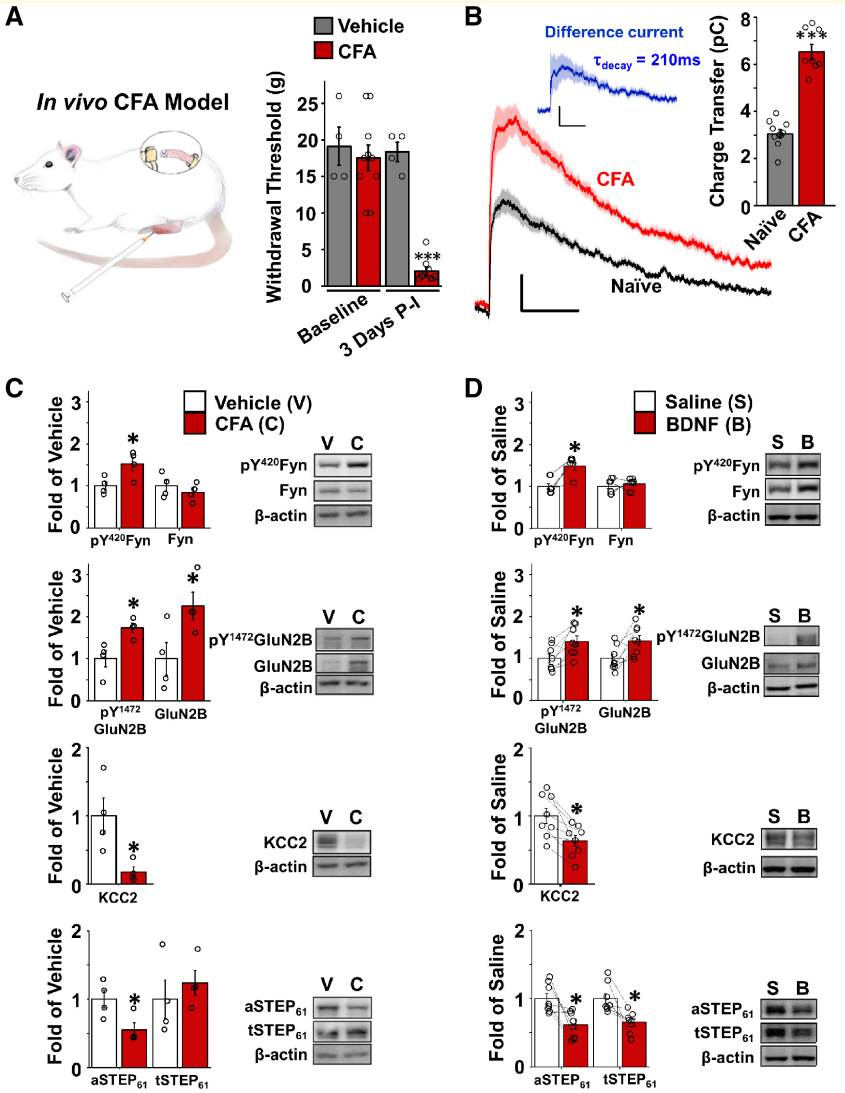

Figure 1 GluN2B NMDARs are potentiated at lamina I synapses in a CFA model of chronic inflammatory pain, with an associated downregulation of synaptic $STEP_{61}$. (**A**) *Left*: Illustration of the *in vivo* CFA injection model of inflammatory pain. The window over the rat's back depicts the area of spine removed for either electrophysiological or biochemical analysis. *Right*: Ipsilateral paw withdrawal threshold (g) at baseline before and 3 days after hindpaw injection with vehicle (grey, $n = 4$, spinal cords used for **C**) or CFA (red, $n = 10$ animals, spinal cords used for **B** and **C**) comparing vehicle to CFA 3 days post-injection. (**B**) *Left*: average NMDAR mEPSCs at +60 mV from lamina I neurons in ipsilateral spinal cord of untreated (black, $n = 10$ cells from eight animals) and CFA-injected (red, $n = 8$ cells from six animals) adult male rats. *Top*: Difference current for NMDAR mEPSCs from CFA rats subtracted from NMDAR mEPSCs from control rats to reveal the 'potentiated' NMDAR mEPSC component. *Right*: Plot of NMDAR charge transfer (from 40 ms to 500 ms) for untreated (grey) versus CFA-injected (red) rats. All current traces in Figs 1, 2 and 4 represented as means (dark lines) ± SEM (lighter bars) of mEPSCs from all averaged cells. Scale bars = 100 ms (*x*-axes); 5 pA (*y*-axes). (**C**) Plots (*left*) and representative western blots (*right*) from synaptosome fractions of ipsilateral superficial dorsal horn from CFA-injected rats (red, $n = 4$) and vehicle-injected rats (white, $n = 4$). For quantification, all targets were normalized to beta-actin as a loading control. (**D**) Plots (*left*) and representative western blots (*right*) from synaptosome fractions of superficial dorsal horn treated with either control saline (white, $n = 8$) or 50 ng/ml recombinant BDNF for 70 min (red, $n = 8$). $^{*}P < 0.05$, $^{**}P < 0.01$ $^{***}P < 0.001$; exact *P*-values can be found in Supplementary Table 3.

using blockers and activators of KCC2-dependent inhibition (Hildebrand *et al.*, 2016), our results suggest that loss of $STEP_{61}$ is necessary and sufficient to prime subsequent potentiation of synaptic NMDARs by BDNF.

Because disinhibition can trigger $STEP_{61}$ downregulation and $STEP_{61}$ regulates Fyn and GluN2B signalling in dorsal horn neurons (Li *et al.*, 2015; Xu *et al.*, 2015*a*, 2018; Azkona *et al.*, 2016), we asked whether loss of $STEP_{61}$ directly couples KCC2-dependent disinhibition to the potentiation of GluN2B NMDARs by Fyn in the *ex vivo* BDNF model of pathological pain. To investigate this, we explored the effects of $STEP_{61}$ antagonists and agonists on superficial

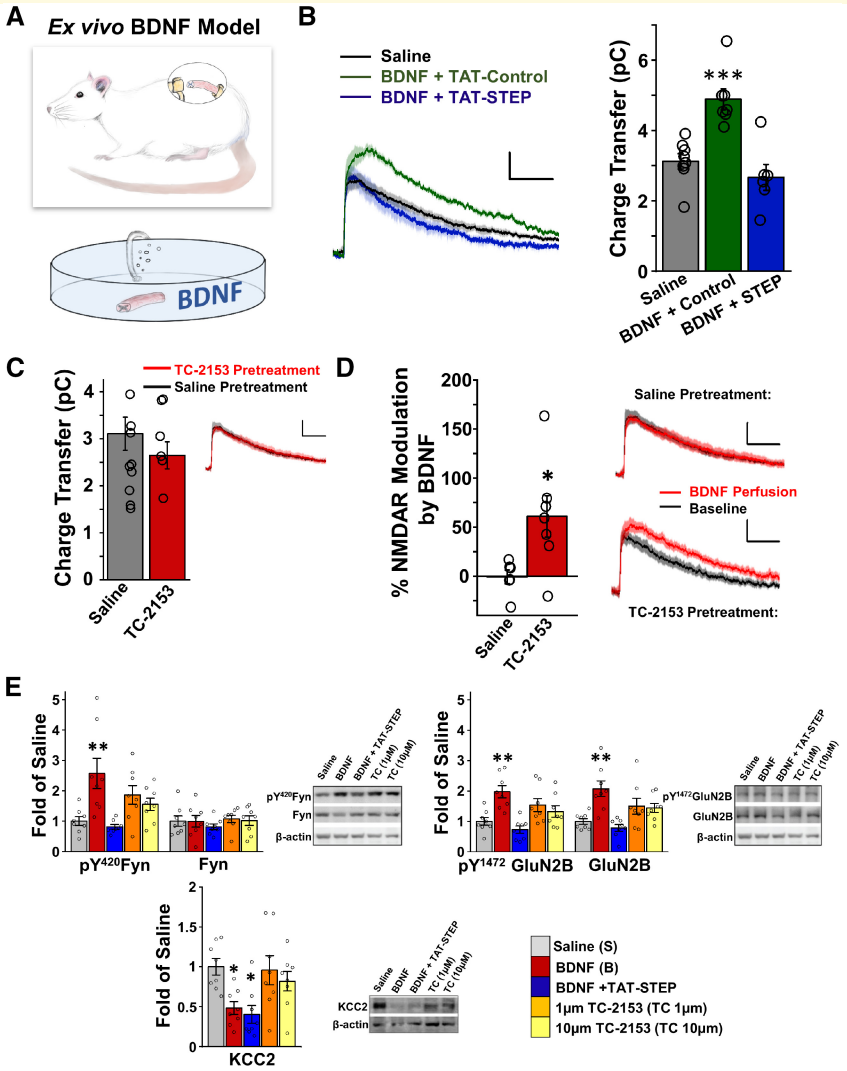

Figure 2 $STEP_{61}$ is necessary and sufficient to prime phosphorylation and potentiation of synaptic GluN2B-NMDARs by BDNF. (**A**) Illustration of the *ex vivo* BDNF model of pathological pain. Sections of lumbar spinal cord (window over rat's back illustrates the lumbar section used) from naïve rats are incubated in oxygenated saline with 50 ng/ml recombinant BDNF for 70 min, before electrophysiology on individual lamina I neurons (**B**–**D**) or biochemistry on superficial dorsal horn tissue (**E**). (**B**) Average NMDAR mEPSC traces (*left*) and associated charge transfer values (*right*) from lamina I neurons of naïve rat spinal slices pretreated with control saline (black, $n = 8$), BDNF and a TAT-control peptide (green, 200 nM, $n = 7$), or BDNF and a membrane permeable active STEP peptide (TAT-STEP; blue, 200 nM, $n = 6$). Scale bars = 100 ms (*x*-axes); 5 pA (*y*-axes). (**C**) Treatment of naïve slices with 1 μM TC-2153 for 70 min (red, $n = 7$) had no significant effect on NMDAR mEPSCs compared to saline-treated slices (grey, $n = 6$). (**D**) Administration of exogenous BDNF (100 ng/ml) during patch-clamp recording caused an increase in NMDAR mEPSC traces in TC-2153 pretreated slices (*bottom right*, $n = 7$), but not in saline pretreated slices (*top right*, $n = 6$). Plot on *left* calculated from NMDAR mEPSC charge transfer after BDNF normalized to baseline charge transfer, for each pretreatment condition. (**E**) Plots and representative western blots from synaptosome fractions of superficial dorsal horn incubated in saline (grey), 50 ng/ml BDNF (red), 50 ng/ml BDNF and 200 nM TAT-STEP (blue), 1 μM TC-2153 (orange), or 10 μM TC-2153 (yellow) for 70 min ($n = 8$ animals/group). For quantification, all targets were normalized to beta actin as a loading control. $^*P < 0.05$, $^{**}P < 0.01$, $^{***}P < 0.001$ compared to saline, exact *P*-values for each comparison can be found in Supplementary Table 3.

dorsal horn synaptosomes from saline- versus BDNF-treated rodent spinal cords. Co-treatment of active TAT-STEP with BDNF prevented the increases in pY^{420} Fyn ($P = 9.9 \times 10^{-4}$), total GluN2B ($P = 2.1 \times 10^{-4}$), and pY^{1472} GluN2B ($P = 1.1 \times 10^{-4}$) that were induced by pretreating naïve spinal slices with BDNF alone ($n = 8$; Fig. 2E). In contrast, co-treatment of TAT-STEP with BDNF did not significantly affect the BDNF-mediated downregulation of KCC2 at superficial dorsal horn synaptosomes ($n = 8$; $P = 0.99$; Fig. 2E). Unlike that observed in cortical neurons (Xu *et al.*, 2014), pretreating spinal sections with the STEP antagonist, TC-2153 (1 μM or 10 μM), did not significantly increase pY^{420} Fyn ($P = 0.66$ for 10 μM), total GluN2B ($P = 0.46$), or pY^{1472} GluN2B ($P = 0.68$) at superficial

dorsal horn synaptosomes compared to saline-treated spinal sections ($n = 8$; Fig. 2E). The finding that blocking $STEP_{61}$ phosphatase activity does not directly induce phosphorylation and potentiation of GluN2B NMDARs by Fyn aligns with our previous observation of minimal basal Src family kinase activity in adult lamina I neurons (Hildebrand *et al.*, 2016). We propose that BDNF is required for a subsequent activation of Fyn kinase. These biochemical experiments (Fig. 2E) suggest that the loss of $STEP_{61}$ links upstream KCC2 downregulation to downstream Fyn-dependent phosphorylation and trafficking of GluN2B NMDARs to superficial dorsal horn synapses during pathological BDNF-dependent pain processing.

To test our working model further, we investigated whether disinhibition is required for BDNF-mediated $STEP_{61}$/Fyn/GluN2B signalling. We used the carbonic acid anhydrase inhibitor, acetazolamide, which blocks disinhibition produced by KCC2-dependent chloride dysregulation without directly altering GABA or glycine receptor-mediated inhibition (Ferrini and De Koninck, 2013; Lee and Prescott, 2015). Co-treatment of spinal sections from naïve rats with acetazolamide (10 μM) and BDNF abolished the BDNF-mediated increases in pY^{420} Fyn ($P = 0.0014$), total GluN2B ($P = 0.0071$), and pY^{1472} GluN2B ($P = 8.1 \times 10^{-4}$) at superficial dorsal horn synaptosomes, while treatment with acetazolamide alone had no significant effects on these targets compared to saline-treated slices ($n = 8$ per group; Fig. 3A and Supplementary Table 3). The effects of BDNF-mediated disinhibition on synaptic NMDARs were restricted to GluN2B, as neither total GluN2A nor tyrosine phosphorylated (pY^{1325}) GluN2A were altered in any of the treatment groups (Fig. 3A). Importantly, co-treatment of acetazolamide with BDNF prevented the decrease in total $STEP_{61}$ at superficial dorsal horn synaptosomes compared to sections treated with BDNF alone ($n = 8$, $P = 0.0047$; Fig. 3A). Thus, blocking KCC2-dependent disinhibition prevents the downregulation of $STEP_{61}$ and subsequent increase in potentiated GluN2B NMDARs by Fyn at superficial dorsal horn synaptosomes in the *ex vivo* BDNF model of pathological pain processing.

We reasoned that if disinhibition is required for a conserved feed-forward pathological pathway, then acetazolamide should also reverse behavioural hypersensitivity induced by persistent inflammation. In CFA-injected rats, administration of acetazolamide significantly reversed the decrease in ipsilateral paw withdrawal threshold ($n = 9$, $P = 4.3 \times 10^{-7}$), while no reversal effect was observed in saline-treated CFA rats ($n = 9$, $P = 0.22$; Fig. 3B). From the totality of our past (Xu *et al.*, 2015*a*; Azkona *et al.*, 2016; Hildebrand *et al.*, 2016; Saavedra *et al.*, 2016) and present evidence, we conclude that loss of $STEP_{61}$ links BDNF/KCC2-dependent disinhibition to the potentiation of GluN2B NMDARs at lamina I synapses in a pathological spinal mechanism that is conserved between chronic inflammatory and neuropathic pain states.

With the exception of a study revealing increased glial activation in the spinal cord of a patient with neuropathic pain (Del Valle *et al.*, 2009), very little is known regarding mechanisms of central sensitization in the human spinal cord. To compound this problem, typical human post-mortem studies rely on delayed tissue collection from autopsy specimens, with associated molecular and cellular degradation. Here we collected lumbar spinal cord tissue from adult male neurological determination of death organ donors within 1 to 3 h (114 ± 25 min, $n = 14$) after aortic cross-clamping, thereby maximizing tissue viability (Fig. 4A). Tissue from donors that had spinal cord damage or medical conditions that could impact spinal pain processing or that were taking chronic pain medications were excluded from the study.

We recorded excitatory synaptic responses from lamina I neurons within transverse sections of human (18- and 52-year-old males; see Supplementary Table 1) spinal cord. NMDAR mEPSCs were significantly ($P = 7.0 \times 10^{-6}$) larger at adult human lamina I synapses ($n = 3$) compared to adult rodent synapses ($n = 10$), with amplitudes and total charge that were more than double that of rodents (Fig. 4B). The decay constant of 204 ± 25 ms ($n = 3$) for NMDAR responses at human lamina I synapses was not significantly different from rodent lamina I synapses (252 ± 26, $n = 10$, $P = 0.36$), and is consistent with GluN2B-mediated NMDAR responses (Hildebrand *et al.*, 2014) (Fig. 4B). In one recording, we were able to sequentially apply antagonists of GluN2A (10 μM TCN-201; Hansen *et al.*, 2012) and then GluN2B (1 μM Ro25–6981; Fischer *et al.*, 1997), which revealed a selective sensitivity of human NMDAR mEPSCs to Ro25–6981 but not TCN-201, as well as a GluN2B-like Ro25–6981-sensitive current (decay rate = 203 ms; Supplementary Fig. 3). Thus, lamina I neurons in the collected human spinal tissue are viable and contain robust synaptic NMDAR responses that are partially mediated by GluN2B-containing receptors.

To test whether the disinhibition-$STEP_{61}$ downregulation-NMDAR potentiation feed-forward pathway occurs at human lamina I synapses, we developed an *ex vivo* BDNF treatment model of human pathological pain processing. As carried out for rodents (Fig. 2A; Coull *et al.*, 2005; Hildebrand *et al.*, 2016), we pretreated adjacent regions of male human (18 to 69 years old) lumbar spinal tissue with saline versus recombinant BDNF (100 ng/ml) for 70 min (Fig. 4A and Supplementary Table 1). Following this, we flash-froze the treated spinal segments and tested for BDNF-mediated changes in expression and phosphorylation of synaptosomal proteins in the superficial dorsal horn versus the remainder of the human spinal cord. Consistent with the rodent *ex vivo* BDNF model (Fig. 1D), we found that BDNF treatment resulted in a significant decrease in KCC2 ($P = 0.044$), total $STEP_{61}$ ($P = 0.019$) and active $STEP_{61}$ ($P = 0.048$) and a significant increase in active Fyn ($P = 0.040$) and pY^{1472} GluN2B ($P = 0.031$) at human superficial dorsal horn synaptosomes

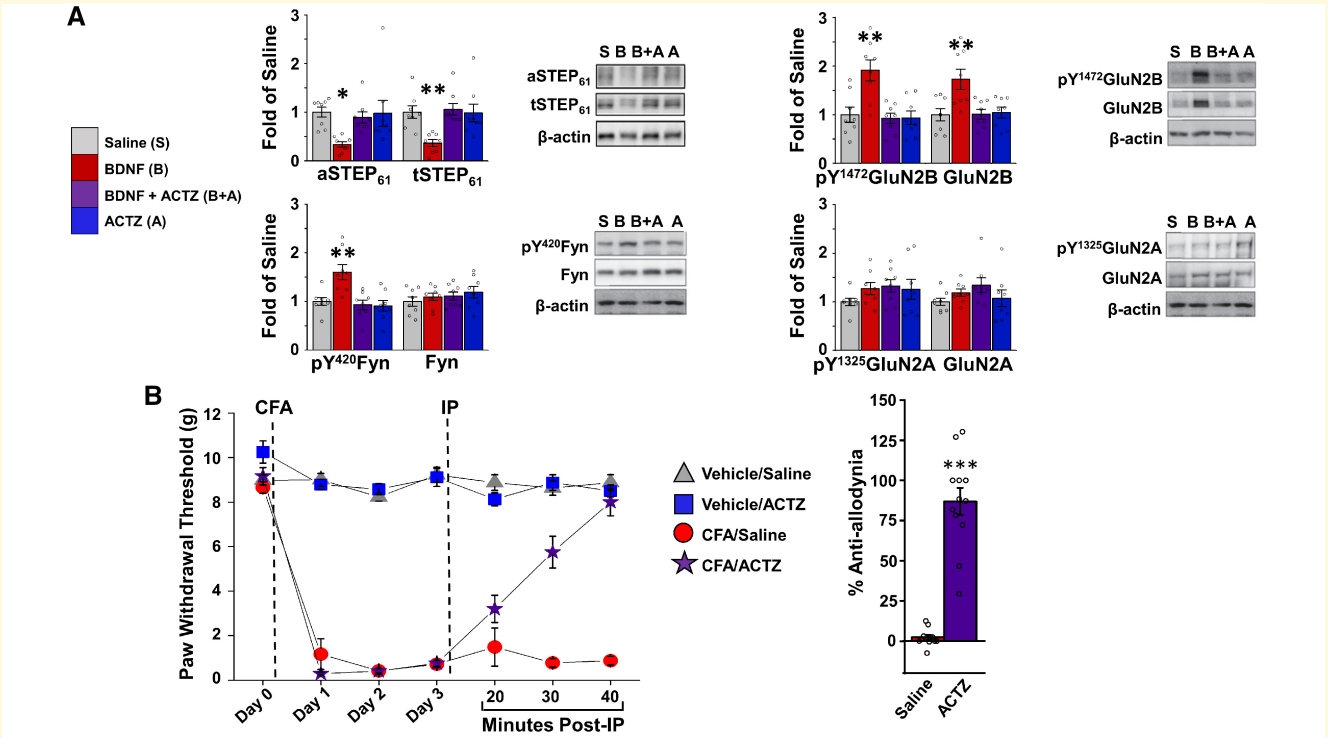

Figure 3 Blocking KCC2-dependent disinhibition attenuates $STEP_{61}$ downregulation by BDNF at superficial dorsal horn synapses and reverses CFA-mediated tactile allodynia. (**A**) Plots and representative western blots from synaptosome fractions of superficial dorsal horn treated with (from *left* to *right*) either saline (grey), BDNF (red), BDNF and acetazolamide (ACTZ) to block KCC2-dependent disinhibition (Lee and Prescott, 2015) (purple), or acetazolamide alone (blue) for 70 min ($n = 8$ animals/group. For quantification, all targets were normalized to beta actin as a loading control. (**B**) *Left*: Ipsilateral paw withdrawal threshold, in grams, of rats before (Day 0) and then 24, 48, and 72 (Day 3) h following a hindpaw injection of either vehicle or CFA. After the Day 3 behaviour testing, either 300 mg/kg acetazolamide or control saline were injected intraperitoneally with behaviour testing 20, 30, and 40 min post-intraperitoneal injection [$n = 8$ for vehicle/saline (grey) and vehicle/acetazolamide (blue), $n = 11$ for CFA/saline (red), and $n = 12$ for CFA/acetazolamide (purple)]. *Right*: Per cent anti-allodynia (reversal of the CFA-dependent decrease in paw withdrawal threshold) 40 min post-intraperitoneal injection of either saline or acetazolamide in CFA-injected rats. $^{*}P < 0.05$, $^{**}P < 0.01$, $^{***}P < 0.001$ compared to saline; exact *P*-values can be found in Supplementary Table 3.

($n = 9$; Fig. 4C, Supplementary Table 3 and Supplementary Fig. 4). This BDNF-mediated pathway was restricted to superficial dorsal horn synaptosomes, as it was not observed in the homogenate fraction of superficial dorsal horn tissue nor at synaptosomes from the remainder of the spinal cord (Supplementary Figs 5 and 6, respectively). Further, we investigated the effect of BDNF on neuronal KCC2 in human *ex vivo* spinal cords of nine male subjects aged from 18 to 64 years old (Fig. 4D–H, Supplementary Fig. 7 and Supplementary Table 1). Superficial dorsal horn neurons were specifically examined based on CGRP immunostaining (Fig. 4D and E). Treatment of human spinal sections with BDNF induced a significant decrease in KCC2 immunostaining at neuronal membranes compared to saline-treated controls (Fig. 4D–G). The BDNF-mediated decrease in membrane KCC2 was paired with a concomitant increase in intracellular KCC2 immunostaining (Fig. 4H). Finally, BDNF treatment increased the proportion of superficial dorsal horn neurons that had KCC2 primarily localized to the intracellular compartment compared to saline-treated tissue (36/108 versus 8/116 respectively, χ^2 test = 61.71; Supplementary Fig. 7).

Discussion

We have discovered that $STEP_{61}$ is the molecular brake that is lost following BDNF-mediated disinhibition at lamina I synapses and subsequently drives the increase in excitatory GluN2B NMDAR responses by BDNF in both rodent and human spinal cords. The coupling between KCC2-dependent disinhibition and NMDAR potentiation is conserved between nerve injury (Hildebrand *et al.*, 2016) and inflammatory models of chronic pain. We therefore propose that this spinal pathway represents a core pathophysiological mechanism that may drive pain hypersensitivity across divergent pain syndromes. Indeed, pharmacological, genetic and biochemical studies have demonstrated that key elements of the pathway—BDNF, KCC2-dependent disinhibition, and GluN2B NMDARs—are essential mediators of pain hypersensitivity in other

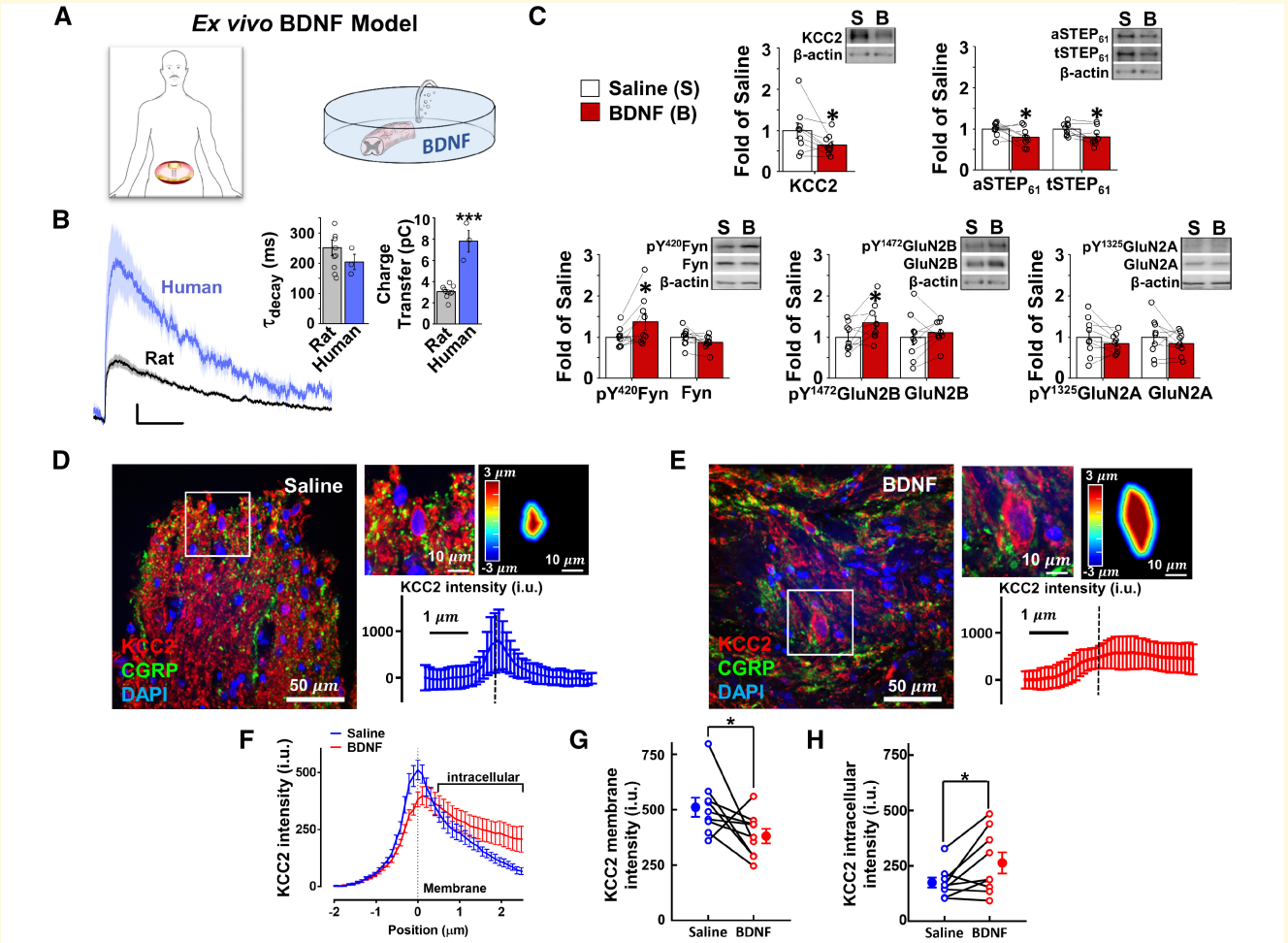

Figure 4 The *ex vivo* BDNF treatment model of pathological pain processing drives a downregulation of KCC2 and $STEP_{61}$ and an increase in pFyn and pGluN2B NMDARs at superficial dorsal horn synapses of viable adult human spinal cord. (**A**) Illustration of the human *ex vivo* BDNF model, highlighting the lumbar section (window). **B**) Average NMDAR mEPSCs at + 60 mV (*left*) from lamina I neurons of human (18 and 52 years old) lumbar or thoracic spinal cord ($n = 3$ neurons) or naïve adult rat lumbar spinal cord ($n = 8$ neurons), with associated decay constant (*middle*) and charge transfer (*right*) values. Scale bars = 100 ms (*x*-axes); 5 pA (*y*-axes). (**C**) Plots and representative western blots from synaptosome fractions of human (30 to 70 years old) superficial dorsal horn treated with either control saline (white, $n = 9$) or 100 ng/ml recombinant BDNF for 70 min (red, $n = 9$). For quantification, all targets were normalized to beta actin as a loading control. (**D** and **E**) *Left*: Representative confocal image of the human superficial dorsal horn incubated in saline (**D**) or BDNF (**E**). KCC2 (red), CGRP (green) and DAPI (blue). A zoomed region (*top middle*) shows a neuron expressing KCC2 together with the delineation of the membrane and the distance to the membrane of each pixel analysed in a colour-coded distance map (*top right*) and KCC2 intensity versus distance to the membrane profile (*bottom*). (**F**) Average KCC2 intensity profiles from superficial dorsal horn neurons incubated in saline (blue) versus BDNF-treated (red) spinal segments of nine male human donors (18–64 years old). (**G** and **H**) Averaged membrane KCC2 intensity values (**G**) and averaged intracellular KCC2 intensity values (**H**) of superficial dorsal horn spinal cord neurons incubated in saline versus BDNF. *$P < 0.05$; exact *P*-values can be found in Supplementary Table 3.

models of chronic pain, including spinal cord injury (Boulenguez *et al.*, 2010; Hama and Sagen, 2012; Kim *et al.*, 2012) and cancer-induced bone pain (Wang *et al.*, 2012; Bao *et al.*, 2014; Hou *et al.*, 2018). However, as a putative molecular hub for spinal pain pathology, heterogeneous signalling factors and mechanisms may differentially interact with the pathway's components. These divergence points mean that no individual molecular player or target is likely to represent a therapeutic solution for all chronic pain syndromes, which may include underlying neuropathic and/or inflammatory mechanisms (Ratté and Prescott, 2016). For example, BDNF is proposed to be primarily released from primary nociceptive afferents following persistent inflammation (Mannion *et al.*, 1999; Zhao *et al.*, 2006; Sikandar *et al.*, 2018) and from activated microglia following nerve injury (Coull *et al.*, 2005; Ulmann *et al.*, 2008), and microglia themselves only mediate lamina I hyperexcitability in the male spinal cord while other immune cells are proposed to drive hyperexcitability in the female spinal cord (Sorge

et al., 2015). Discriminating between divergent and convergent pain signalling elements will be needed to develop generalized versus syndrome-specific therapeutic strategies.

Given the plethora of molecular targets that continue to emerge as spinal mechanisms of pain are investigated, an essential missing step in the clinical development of novel therapeutics is to validate which candidates contribute to human spinal pain pathology. To address this, we have developed an *ex vivo* human BDNF treatment model of pathological pain processing that is based on an established approach for rodent spinal cord. In the rodent model, *ex vivo* BDNF treatment induces the same changes in protein composition and excitatory responses at lamina I synapses as that observed in the *in vivo* rodent models of chronic inflammatory and neuropathic pain (Coull *et al.*, 2005; Hildebrand *et al.*, 2016). Similar to this *ex vivo* rodent model, we are able to collect human spinal tissue that is neuro-protected right up until the point of collection. Using sectioned human dorsal horn tissue, we have characterized functional excitatory synaptic responses from individual lamina I neurons and have shown that phosphorylation-dependent intracellular signalling pathways can be activated by BDNF *ex vivo*, supporting the conclusion that the dorsal horn nociceptive network remains highly viable. Indeed, by combining the human *ex vivo* BDNF model with rodent *ex vivo* and *in vivo* pain models, we have shown that $STEP_{61}$ is the molecular determinant that is lost to drive coupling between BDNF-mediated disinhibition and facilitation of GluN2B NMDARs at both rodent and human lamina I synapses. Future experiments will test what molecular players link KCC2-dependent disinhibition to decreased $STEP_{61}$ activity, and whether the role of candidates such as PKA (Xu *et al.*, 2015*b*; Poddar *et al.*, 2016) are conserved in pathological coupling mechanisms between rodent and human pain models. Using this approach, we can validate the role of identified molecular candidates in human spinal tissue and then test how targeting these players *in vivo* impacts pain hypersensitivity in rodent models of specific pain syndromes.

Acknowledgements

We thank Drs Tuan Trang and Hongyu Sun for providing critical feedback on the manuscript. We thank the families that consented to donation of their loved one's spinal tissue for research; this gift is greatly appreciated. We also thank Dr Suzan Chen and Lei Zhou, our clinical research coordinators, for their help organizing the human tissue collection, and Dr Diana Ghinda and the operating room staff at The Ottawa Hospital for aiding with human tissue collection.

Funding

This study was supported by a John R. Evans Leaders Fund grant from the Canada Foundation for Innovation (M.E.H.), a Discovery Grant from the Natural Sciences and Engineering Research Council of Canada (M.E.H.), an Early Career Research Grant from the International Association for the Study of Pain (M.E.H.; A.G.G), an Early Career Investigator Pain Research Grant from the Canadian Pain Society and Pfizer Canada (M.E.H.), and Project/Operating Grants from the Canadian Institutes of Health Research (M.E.H., 388432; Y.D.K., 12942).

Competing interests

The authors report no competing interests.

Supplementary material

Supplementary material is available at *Brain* online.

References

Abe T, Matsumura S, Katano T, Mabuchi T, Takagi K, Xu L, et al. Fyn kinase-mediated phosphorylation of NMDA receptor NR2B subunit at Tyr1472 is essential for maintenance of neuropathic pain. Eur J Neurosci 2005; 22: 1445–54.

Alles SRA, Smith PA. Etiology and pharmacology of neuropathic pain. Pharmacol Rev 2018; 70: 315–47.

Azkona G, Saavedra A, Aira Z, Aluja D, Xifró X, Baguley T, et al. Striatal-enriched protein tyrosine phosphatase modulates nociception: evidence from genetic deletion and pharmacological inhibition. Pain 2016; 157: 377–86.

Bao Y, Hou W, Liu R, Gao Y, Kong X, Yang L, et al. PAR2-mediated upregulation of BDNF contributes to central sensitization in bone cancer pain. Mol Pain 2014; 10: 28.

Bonin RP, Bories C, De Koninck Y. A simplified up-down method (SUDO) for measuring mechanical nociception in rodents using von Frey filaments. Mol Pain 2014; 10: 26.

Boulenguez P, Liabeuf S, Bos R, Bras H, Jean-Xavier C, Brocard C, et al. Down-regulation of the potassium-chloride cotransporter KCC2 contributes to spasticity after spinal cord injury. Nat Med 2010; 16: 302–07.

Bourinet E, Altier C, Hildebrand ME, Trang T, Salter MW, Zamponi GW. Calcium-permeable ion channels in pain signaling. Physiol Rev 2014; 94: 81–140.

Coull JAM, Beggs S, Boudreau D, Boivin D, Tsuda M, Inoue K, et al. BDNF from microglia causes the shift in neuronal anion gradient underlying neuropathic pain. Nature 2005; 438: 1017–21.

Del Valle L, Schwartzman RJ, Alexander G. Spinal cord histopathological alterations in a patient with longstanding complex regional pain syndrome. Brain Behav Immun 2009; 23: 85–91.

Ferrini F, De Koninck Y. Microglia control neuronal network excitability via BDNF signalling. Neural Plast. 2013; 2013: 1–11.

Ferrini F, Lorenzo L-E, Godin AG, Quang M Le, De Koninck Y. Enhancing KCC2 function counteracts morphine-induced hyperalgesia. Sci Rep 2017; 7: 3870.

Fischer G, Mutel V, Trube G, Malherbe P, Kew JN, Mohacsi E, et al. Ro 25–6981, a highly potent and selective blocker of N-methyl-D-aspartate receptors containing the NR2B subunit. Characterization in vitro. J Pharmacol Exp Ther 1997; 283: 1285–92.

Gereau RW, Sluka KA, Maixner W, Savage SR, Price TJ, Murinson BB, et al. A pain research agenda for the 21st century. J Pain 2014; 15: 1203–14.

Gibson SJ, Polak JM, Bloom SR, Sabate IM, Mulderry PM, Ghatei MA, et al. Calcitonin gene-related peptide immunoreactivity in the

spinal cord of man and of eight other species. J Neurosci 1984; 4: 3101–11.

Hama A, Sagen J. Combinations of intrathecal gamma-amino-butyrate receptor agonists and N-methyl-d-aspartate receptor antagonists in rats with neuropathic spinal cord injury pain. Eur J Pharmacol 2012; 683: 101–8.

Hansen KB, Ogden KK, Traynelis SF. Subunit-selective allosteric inhibition of glycine binding to NMDA receptors. J Neurosci 2012; 32: 6197–208.

Hildebrand ME, Pitcher GM, Harding EK, Li H, Beggs S, Salter MW. GluN2B and GluN2D NMDARs dominate synaptic responses in the adult spinal cord. Sci Rep 2014; 4: 4094.

Hildebrand ME, Xu J, Dedek A, Li Y, Sengar AS, Beggs S, et al. Potentiation of synaptic GluN2B NMDAR currents by Fyn kinase is gated through BDNF-mediated disinhibition in spinal pain processing. Cell Rep 2016; 17: 2753–65.

Hou X, Weng Y, Wang T, Ouyang B, Li Y, Song Z, et al. Suppression of HDAC2 in spinal cord alleviates mechanical hyperalgesia and restores KCC2 expression in a rat model of bone cancer pain. Neuroscience 2018; 377: 138–49.

Hunt SP, Rossi J. Peptide- and non-peptide-containing unmyelinated primary afferents: the parallel processing of nociceptive information. Philos Trans R Soc Lond B Biol Sci 1985; 308: 283–9.

Ju G, Hökfelt T, Brodin E, Fahrenkrug J, Fischer JA, Frey P, et al. Primary sensory neurons of the rat showing calcitonin gene-related peptide immunoreactivity and their relation to substance P-, somatostatin-, galanin-, vasoactive intestinal polypeptide- and cholecystokinin-immunoreactive ganglion cells. Cell Tissue Res 1987; 247: 417–31.

Kim Y, Cho H, Ahn YJ, Kim J, Yoon YW. Effect of NMDA NR2B antagonist on neuropathic pain in two spinal cord injury models. Pain 2012; 153: 1022–29.

Kuner R. Spinal excitatory mechanisms of pathological pain. Pain 2015; 156: S11–7.

Latremoliere A, Woolf CJ. Central sensitization: a generator of pain hypersensitivity by central neural plasticity. J Pain 2009; 10: 895–926.

Lee KY, Prescott SA. Chloride dysregulation and inhibitory receptor blockade yield equivalent disinhibition of spinal neurons yet are differentially reversed by carbonic anhydrase blockade. Pain 2015; 156: 2431–37.

Li L, Shi L, Xu Y-M, Yang X, Suo Z-W, Hu X-D. GABAergic inhibition regulated pain sensitization through STEP61 signaling in spinal dorsal horn of mice. Anesthesiology 2015; 122: 686–97.

Mannion RJ, Costigan M, Decosterd I, Amaya F, Ma QP, Holstege JC, et al. Neurotrophins: peripherally and centrally acting modulators of tactile stimulus-induced inflammatory pain hypersensitivity. Proc Natl Acad Sci 1999; 96: 9385–90.

Mercado A, Broumand V, Zandi-Nejad K, Enck AH, Mount DB. A C-terminal domain in KCC2 confers constitutive K + -Cl- cotransport. J Biol Chem 2006; 281: 1016–26.

Morgan P, Van Der Graaf PH, Arrowsmith J, Feltner DE, Drummond KS, Wegner CD, et al. Can the flow of medicines be improved? Fundamental pharmacokinetic and pharmacological principles toward improving Phase II survival. Drug Discov Today 2012; 17: 419–24.

Paul S, Olausson P, Venkitaramani DV, Ruchkina I, Moran TD, Tronson N, et al. The striatal-enriched protein tyrosine phosphatase gates long-term potentiation and fear memory in the lateral amygdala. Biol Psychiatry 2007; 61: 1049–61.

Poddar R, Rajagopal S, Shuttleworth CW, Paul S. Zn2 + -dependent activation of the trk signaling pathway induces phosphorylation of the brain-enriched tyrosine phosphatase STEP: molecular basis for ZN2 + -induced ERK MAPK activation. J Biol Chem 2016; 291: 813–25.

Ratté S, Prescott SA. Afferent hyperexcitability in neuropathic pain and the inconvenient truth about its degeneracy. Curr Opin Neurobiol 2016; 36: 31–7.

Ren K, Hylden JLK, Williams GM, Ruda MA, Dubner R. The effects of a non-competitive NMDA receptor antagonist, MK-801, on behavioral hyperalgesia and dorsal horn neuronal activity in rats with unilateral inflammation. Pain 1992; 50: 331–44.

Rosenfeld MG, Mermod J-J, Amara SG, Swanson LW, Sawchenko PE, Rivier J, et al. Production of a novel neuropeptide encoded by the calcitonin gene via tissue-specific RNA processing. Nature 1983; 304: 129–35.

Saavedra A, Puigdellívol M, Tyebji S, Kurup P, Xu J, Ginés S, et al. BDNF induces striatal-enriched protein tyrosine phosphatase 61 degradation through the proteasome. Mol Neurobiol 2016; 53: 4261–73.

Sikandar S, Minett MS, Millet Q, Santana-Varela S, Lau J, Wood JN, et al. Brain-derived neurotrophic factor derived from sensory neurons plays a critical role in chronic pain. Brain 2018; 141: 1028–39.

Sorge RE, Mapplebeck JCS, Rosen S, Beggs S, Taves S, Alexander JK, et al. Different immune cells mediate mechanical pain hypersensitivity in male and female mice. Nat Neurosci 2015; 18: 1081–3.

Todd AJ. Neuronal circuitry for pain processing in the dorsal horn. Nat Rev Neurosci 2010; 11: 823–36.

Trepanier CH, Jackson MF, MacDonald JF. Regulation of NMDA receptors by the tyrosine kinase Fyn. FEBS J 2012; 279: 12–9.

Ulmann L, Hatcher JP, Hughes JP, Chaumont S, Green PJ, Conquet F, et al. Up-regulation of P2X4 receptors in spinal microglia after peripheral nerve injury mediates BDNF release and neuropathic pain. J Neurosci 2008; 28: 11263–68.

Wang L-N, Yang J-P, Ji F, Zhan Y, Jin X, Xu Q-N, et al. Brain-derived neurotrophic factor modulates N-methyl-D-aspartate receptor activation in a rat model of cancer-induced bone pain. J Neurosci Res 2012; 90: 1249–60.

Williams JR, Sharp JW, Kumari VG, Wilson M, Payne JA. The neuron-specific K-Cl cotransporter, KCC2. Antibody development and initial characterization of the protein. J Biol Chem 1999; 274: 12656–64.

Xu J, Chatterjee M, Baguley TD, Brouillette J, Kurup P, Ghosh D, et al. Inhibitor of the tyrosine phosphatase STEP reverses cognitive deficits in a mouse model of Alzheimer's disease. PLoS Biol 2014; 12: e1001923.

Xu J, Kurup P, Foscue E, Lombroso PJ. Striatal-enriched protein tyrosine phosphatase regulates the PTPα/Fyn signaling pathway. J Neurochem 2015a; 134: 629–41.

Xu J, Kurup P, Nairn AC, Lombroso PJ. Synaptic NMDA receptor activation induces ubiquitination and degradation of STEP61. Mol Neurobiol 2018; 55: 3096–111.

Xu J, Kurup P, Zhang Y, Goebel-Goody SM, Wu PH, Hawasli AH, et al. Extrasynaptic NMDA receptors couple preferentially to excitotoxicity via calpain-mediated cleavage of STEP. J Neurosci 2009; 29: 9330–43.

Xu YM, Wang XT, Zhang ZY, Suo ZW, Yang X, Hu XD. Noradrenergic α2 receptor attenuated inflammatory pain through STEP61/ERK signalling. Eur J Pain 2015b; 19: 1298–1307.

Yekkirala AS, Roberson DP, Bean BP, Woolf CJ. Breaking barriers to novel analgesic drug development. Nat Rev Drug Discov 2017; 16: 545–64.

Zhao J, Seereeram A, Nassar MA, Levato A, Pezet S, Hathaway G, et al. Nociceptor-derived brain-derived neurotrophic factor regulates acute and inflammatory but not neuropathic pain. Mol Cell Neurosci 2006; 31: 539–48.